

Spin dynamics in the $S = \frac{1}{2}$ quantum kagome compound vesignieite, $\text{Cu}_3\text{Ba}(\text{VO}_5\text{H})_2$

R. H. Colman,¹ F. Bert,² D. Boldrin,¹ A. D. Hillier,³ P. Manuel,³ P. Mendels,² and A. S. Wills^{1,*}

¹*Department of Chemistry, University College London, 20 Gordon Street, London, WC1H 0AJ, United Kingdom*

²*Laboratoire de Physique des Solides, UMR CNRS 8502, Université Paris-Sud, 91405 Orsay, France*

³*ISIS Facility, STFC, Rutherford Appleton Laboratory, Chilton, Oxfordshire OX11 0QX, United Kingdom*

(Received 20 January 2011; revised manuscript received 13 April 2011; published 31 May 2011)

We report the study of high-quality samples of the frustrated $S = \frac{1}{2}$ kagome antiferromagnet vesignieite, $\text{Cu}_3\text{Ba}(\text{VO}_5\text{H})_2$. Neutron powder diffraction measurements evidence the excellence of the kagome lattice and show no sign of a transition to magnetic long-range order. A kink in the susceptibility below $T = 9$ K is matched to a reduction in paramagnetic-like correlations in the diffraction data and a slowing of the spin dynamics observed by μSR . Our results point to an exotic quantum state below 9 K with coexistence of both dynamical and small frozen moments $\sim 0.1\mu_B$. We propose that this novel quantum ground state is stabilized by a large Dzyaloshinsky-Moriya interaction.

DOI: [10.1103/PhysRevB.83.180416](https://doi.org/10.1103/PhysRevB.83.180416)

PACS number(s): 75.40.Gb, 76.75.+i

The low connectivity and dimensionality of a kagome lattice of antiferromagnetically coupled $S = \frac{1}{2}$ ions (KAFM) make it the ideal framework to study the highly sought after quantum spin liquid (QSL) state.^{1–4} Despite the advances in theoretical understanding of QSLs, progress in the field is hindered by a lack of physical examples of $S = \frac{1}{2}$ KAFMs. Even the best model systems possess noteworthy shortcomings, such as structural distortions, disorder, and further neighbor exchange.

Much of the interest in KAFMs was inspired by evidence of a liquid-like ground state in the kagome-like compound $\text{SrCr}_9\text{pGa}_{12-9\text{p}}\text{O}_{19}$ (SCGO) where persistent spin dynamics were observed down to 100 mK using muon spin relaxation spectroscopy (μSR), far below a spin-glass transition at $T_g \simeq 3.5$ K.⁵ Following from this work, volborthite, $\text{Cu}_3\text{V}_2\text{O}_7(\text{OH})_2 \cdot 2(\text{H}_2\text{O})$, was believed for several years to be the closest approximation to a $S = \frac{1}{2}$ KAFM. Susceptibility measurements showed it to have strong antiferromagnetically coupled spins ($\theta_w = -115$ K)⁶ that remain dynamic as $T \rightarrow 0$,⁷ despite partial spin freezing.⁸ This lack of Néel order is remarkable given the monoclinic distortion to the lattice: the triangles of volborthite are isosceles and the inequivalence of the Cu–O–Cu superexchange pathways is expected to reduce the ground-state degeneracy.

Undistorted kagome lattices of $S = \frac{1}{2}$ ions have been studied more recently in several closely related materials: Zn and Mg herbertsmithites, kapellasite and haydeite.^{9–14} These systems display the characteristic properties of frustrated magnets, such as suppression of magnetic ordering,^{13,15,16} and have revealed new effects such as temperature-independent magnetic excitation spectra.¹⁷ However, they all also feature some degree of dilution of the moment-bearing Cu^{2+} ions by diamagnetic metal ions ($\text{Zn}^{2+}/\text{Mg}^{2+}$) that complicates understanding of the ground-state properties.^{9,14,18,19}

In order to differentiate the intrinsic properties of the KAFM from the effects caused by deviations from ideality, new model materials close to the idealized $S = \frac{1}{2}$ kagome structure are needed. One recently proposed example is the mineral vesignieite, $\text{Cu}_3\text{Ba}(\text{VO}_5\text{H})_2$.^{20–22} In this material, the kagome net is not created by diamagnetic dilution of another lattice,

and so there is little possibility of anion exchange leading to structural defects within the KAFM.

In this Rapid Communication, we investigate high-quality samples of vesignieite by powder neutron diffraction, magnetic susceptibility, and μSR spectroscopy. We show that the kagome lattice is very close to the ideal geometry and therefore that vesignieite provides an opportunity for the study of minimally perturbed KAFM physics (see Fig. 1).

No structural refinements were presented of the previously synthesized samples of vesignieite.²⁰ Inspection of the broad powder x-ray diffraction (XRD) peaks, however, indicates that they are poorly crystalline, with coherent order restricted to length scales as low as a few nanometers. Such deficiency will disrupt the magnetic behavior of the KAFM and complicate its interpretation.

We used an alternative synthetic method, based on the evaporation of ammonia from a solution of Schweizer's reagent,²³ $[\text{Cu}(\text{NH}_3)_4(\text{H}_2\text{O})_2](\text{OH})_2$ (0.678 g $\text{Cu}(\text{OH})_2$ in 100 ml 28 % NH_4OH solution), vanadium pentoxide, V_2O_5 (0.154 g), and barium acetate, $\text{Ba}(\text{CH}_3\text{COO})_2$ (0.217 g), heated to reflux for ~ 4 h. The evaporation of ammonia causes the slow release of $\text{Cu}(\text{OH})_2$ into solution and the controlled crystallization of vesignieite. To further improve crystallinity, the vesignieite sample (~ 1 g) was then hydrothermally annealed in 25 ml of H_2O (or 99.9 atom% D_2O for the deuterated sample), at 190 °C, for 48 h. The resultant vesignieite sample was found to be phase pure by powder XRD.

Powder neutron diffraction (PND) data were collected between 1.5 K and 50 K on a deuterated sample of vesignieite, $\text{Cu}_3\text{Ba}(\text{VO}_5\text{D})_2$ (1.75 g), using the diffractometer WISH (ISIS, UK). Rietveld refinements of the crystal structure of vesignieite afforded the fit shown in Fig. 2. Our refined parameters show that the isosceles triangle built from the Cu(1) and Cu(2) sites is very close to equilateral with $r_1 = 2.949(1)\text{Å}$ and $r_2 = 2.951(1)\text{Å}$. This distortion of 0.07% is far less than that of previous samples²⁰ and greatly strengthens the case for vesignieite as an important model system with which to probe $S = \frac{1}{2}$ kagome physics.

Over the range 1.5–50 K, no change was seen in the Bragg diffraction other than a small thermal lattice contraction; there was no evidence of magnetic-Bragg diffraction or

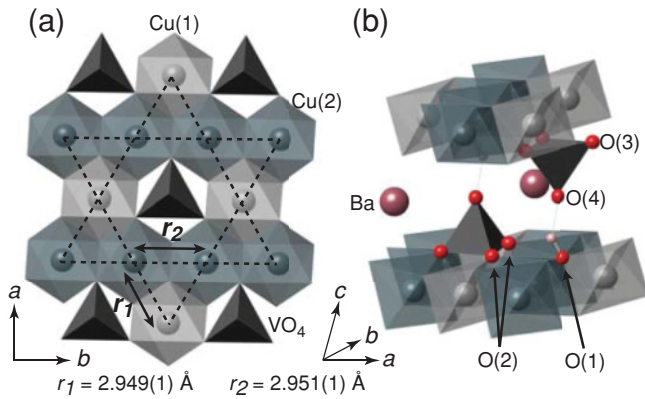


FIG. 1. (Color online) The kagome lattice of vesignieite has two crystallographically distinct CuO_6 octahedra and near three-fold rotational symmetry. The kagome planes are coupled by VO_4 tetrahedra, hydrogen bonded to hydroxyl groups in the neighboring planes, and interstitial Ba^{2+} ions. There are four types of oxygen positions: O1, the hydrogen bonding O–H group; O2 and O3 define the basal plane of the VO_4 tetrahedra; and O4 is the tetrahedral apex.

broad features indicative of short-range spin correlations. Remarkably, a reduction in the form-factor-type scattering at high d spacing is observed below $T \sim 10$ K, indicating that below this temperature the paramagnetic-like component is being reduced although no other magnetic scattering is seen to develop [Fig. 2(b)].

DC-magnetic susceptibility measurements were performed using a Quantum Design MPMS SQUID magnetometer. In the region $100 < T < 300$ K, for applied field $\mu_0 H > 1$ T, the data display a typical Curie-Weiss response that could be fitted to give a Weiss temperature $\theta_W = -85(5)$ K, indicative of antiferromagnetic exchange, and an effective moment $\mu_{\text{eff}} = 2.02(2) \mu_B$ in agreement with published data.²⁰ As in Ref. 20, a kink in the susceptibility is observed at $T \sim 9$ K. Our data show that this feature is also accompanied by bifurcation of the field-cooled and zero-field-cooled branches (Fig. 3), which is most obvious at low field and is suggestive of spin-glass-like freezing.

As a local probe, μSR is a technique of choice to discriminate between extrinsic and intrinsic magnetic contributions. It has proven to be a powerful tool for probing spin dynamics in frustrated materials and in the search for spin liquid ground states. A protonated sample of vesignieite was investigated using the spectrometer MUSR (ISIS, UK). As muons, μ^+ , implant near centers of negative charge, the four crystallographically distinct oxygen positions in vesignieite (O1–O4, Fig. 1) give rise to four likely stopping positions.

For $T > 9$ K, the muon relaxation is dominated by the nuclear magnetism of Cu, V, and H nuclei, which is static at the muon time scale. Muons also experience the Cu^{2+} electronic spin dynamics, modeled by an additional slow exponential decay. For required simplicity, the same relaxation rate, λ , for all muon sites was imposed. The zero-field asymmetries (Fig. 4) were therefore fitted to $P_{\text{para}}(t) = P_{\text{nuc}}(t)e^{-\lambda t}$ where the temperature-independent P_{nuc} is the static nuclear contribution.²⁴ Above $T = 15$ K, an almost temperature-independent rate $\lambda = 0.012(1) \mu\text{s}^{-1}$ was seen, which arises from exchange fluctuations of the Cu^{2+} electronic

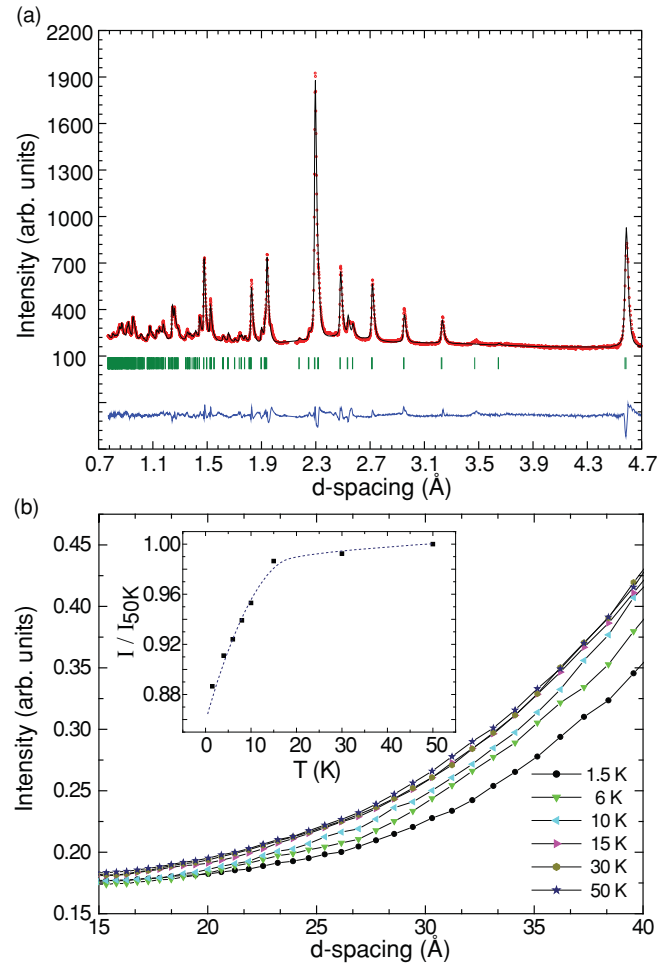


FIG. 2. (Color online) (a) PND data collected from a deuterated vesignieite sample at $T = 1.5$ K. The red points are the data, the black line is the fit, the blue curve is the difference, and the tick marks indicate reflection positions. Refined lattice parameters, in the monoclinic space group $C 12/m 1$ (no. 12) are $a = 10.210(2)$ Å, $b = 5.903(1)$ Å, $c = 7.739(1)$ Å, and $\beta = 116.15(1)^\circ$. The final R_{wp} is 3.61. Based on collinear antiferromagnetic models, *e.g.*, $\mu(\text{Cu}_1) = 2m_{\parallel b}$ and $\mu(\text{Cu}_2) = \mu(\text{Cu}_3) = -m_{\parallel b}$, we estimate an average sublattice magnetization of $>0.4 \mu_B$ would need to occur to become apparent in these data. (b) Plot of the high d -spacing data at several temperatures. Inset: integrated intensity of the scattering in the range $15 < d < 40$ Å as a function of temperature, normalized to the 50 K scattering. The dashed line is a guide to the eye.

spins with the rate $\nu \simeq J/2\hbar^5$. When $J/k_B = 53$ K is used,²⁰ the relaxation in the paramagnetic limit $\lambda = 2\Delta H/\nu$ yields the width $\Delta H \simeq 0.15$ T for the random field distribution at the muon sites. This value is in fair agreement with the crude estimate of the average dipolar field $\simeq 0.12$ T arising from the fluctuating $\simeq 1 \mu_B$ copper moments and experienced by muons located close to the oxygen sites.

Below $T \sim 9$ K, the relaxation of the asymmetry steeply increases, a change that cannot be accounted for simply by a slowing down of the electronic spin dynamics. In addition, a fast initial relaxation develops, and the polarization as $t \rightarrow \infty$ is no longer 0. These are the usual signatures of the presence of a magnetic phase, static on the muon time scale. To gain

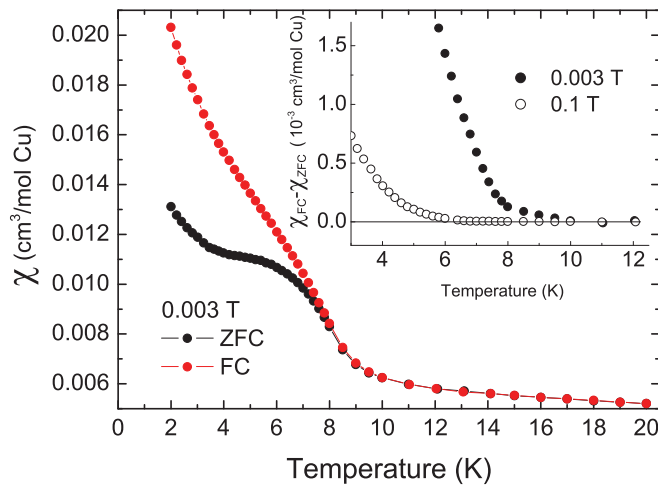


FIG. 3. (Color online) (a) The temperature-dependent zero-field-cooled (ZFC) and field-cooled (FC) DC susceptibility measured in a field of 0.003 T. Inset: difference of the ZFC and FC susceptibilities.

more insight into the nature of this frozen phase, spectra were recorded at $T = 1.5$ K on the GPS instrument at the Paul Scherrer Institut facility (CH), which provides high resolution at short times (see inset of Fig. 4). The absence of spontaneous oscillations in the zero-field muon polarization decay points to a highly disordered magnetic state of the spin-glass type, which is consistent with the absence of magnetic-Bragg peaks in PND. Moreover, a field applied along the initial muon polarization direction of ~ 0.1 T is required to overcome the internal static field distribution. This indicates that the maximal static internal field at the muon sites is ~ 0.01 T. This value is in contrast to the former estimation of the dipolar field ~ 0.12 T generated by full $1\text{-}\mu_B$ copper moments. We deduce that the frozen moments in the static phase are surprisingly small, of the order of $0.1 \mu_B$. This suggests that not all the spin degrees of freedom are freezing below 9 K or that strong quantum fluctuations are present in the frozen phase.

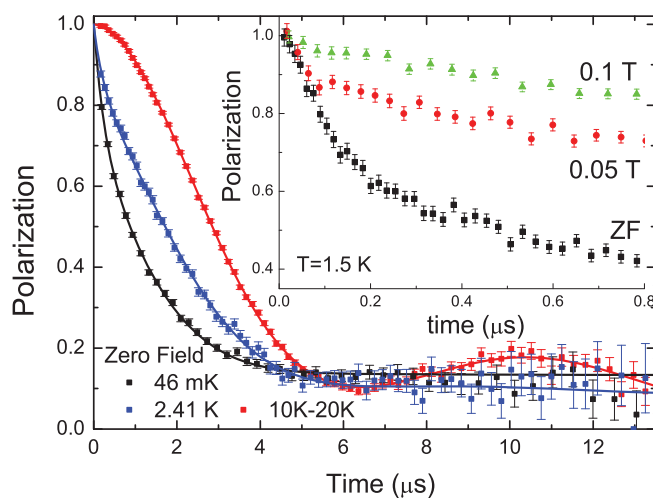


FIG. 4. (Color online) Muon decay asymmetry vs time in zero applied field. Inset: initial asymmetry at 1.5 K in zero and longitudinal fields.

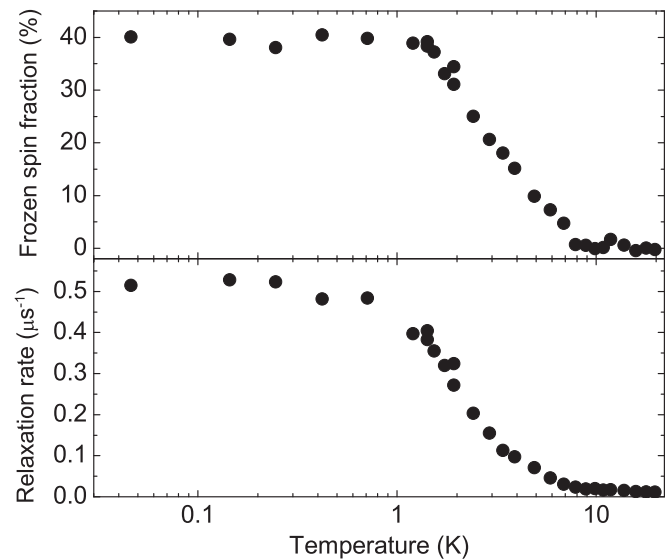


FIG. 5. Temperature dependence of the frozen spin fraction f_f and the muon relaxation rate λ determined from the fits of the zero-field asymmetries (see text).

The muon asymmetry across the whole temperature range could be fitted with the function $P(t) = f_f P_f(t) + (1 - f_f) P_{\text{para}}(t)$, where f_f monitors the fraction of spins involved in the frozen magnetic phase. Given the limited accuracy at short time of the ISIS data, the minimal temperature independent form $P_f(t) = \frac{2}{3} e^{-t\lambda_{\text{fast}}} + \frac{1}{3}$, where $\lambda_{\text{fast}} = 4(1) \mu\text{s}^{-1}$, was used to account for the static spin fraction. The frozen fraction, f_f , is found to increase gradually below $T = 9$ K at the expense of the paramagnetic, nonfrozen, fraction [see Fig. 5(a)] down to $T \sim 1$ K, where it saturates at $\sim 40\%$ of the sample spins. Simultaneously, the relaxation in the nonfrozen phase gradually increases on cooling below $T = 9$ K and eventually saturates at $\lambda = 0.50(2) \mu\text{s}^{-1}$ below 1 K [see Fig. 5(b)], indicating persistent, slow dynamics as $T \rightarrow 0$. Although the origin of this behavior remains unclear, it is reminiscent of many other frustrated antiferromagnetic systems such as kagome bilayers,⁵ volborthite,⁷ or even rare-earth pyrochlores²⁶ and points to an exotic quantum ground state in the unfrozen spin fraction of the sample. The similar temperature evolutions of the frozen fraction, f_f , and the relaxation rate, λ , in the paramagnetic phase indicates that these two responses are within the same framework and neither is an extrinsic (impurity) effect. Our μSR results clearly demonstrate that below 9 K the spin dynamics of *all* Cu^{2+} are strongly suppressed, with $\sim 40\%$ of them freezing. This rules out the previous interpretation of the 9-K upturn in the susceptibility, as arising from 7% free impurity spins.²⁰ The 9-K feature in the μSR data instead points to the building up of intrinsic spin-spin correlations in vesignite.

In summary, structural refinements of PND data show high-quality samples of vesignite to have near three-fold rotation symmetry of the idealized magnetic kagome lattice. Susceptibility, diffraction data, and μSR data consistently evidence a strong slowing of the spin dynamics below 9 K, down to weak static magnetism for $\sim 40\%$ of the Cu spins. It is enlightening to compare the exotic ground-state properties of

vesignieite to other well-studied quantum kagome materials. In structurally perfect herbertsmithite, where all Cu^{2+} ions are related by three-fold symmetry, no transition to a static state, even of a small spin fraction, is detected down to at least $J/4000$.¹⁵ In volborthite, where the kagome lattice is sizeably distorted $\sim 3\%$,^{6,20} partial static magnetism was detected in NMR and SQUID measurements below $\sim J/80$, while μSR relaxation was found to be dominated by coexisting spin dynamics. In this context, it is surprising to observe a spin state reminiscent of that in volborthite in the quasiperfect kagome material vesignieite at a high temperature of $\sim J/6$. At the classical level, distortion of the kagome lattice hinders the connection of the degenerated ground states by local zero-energy modes and may favor spin glass physics.²⁷ It seems, however, unlikely that the minute distortion of $\sim 0.07\%$ in vesignieite is responsible for partial freezing at $\sim J/6$. The Dzyaloshinsky-Moriya interaction, which is allowed to occur on the kagome lattice, is another possible perturbation to the pure KAFM. It may destabilize the kagome spin liquid ground state if its magnitude, D , is $D/J \gtrsim 0.1$.²⁸ Analysis of the ESR line width has provided the value $0.044 < D/J < 0.08$ for herbertsmithite.^{29,30} Although a detailed understanding

of the ESR line shape is quite involved, we may assume a similar origin of the room-temperature width $\Delta H \sim D^2/J$ also in vesignieite. Given that ΔH is close to the value seen in herbertsmithite,²¹ while J is three times smaller, we calculate that D/J would be ~ 0.14 , that is, on the Néel ordered side of the predicted critical point.²⁹ Further studies are needed to ascertain the exact ratio of D/J and to understand why long-range order is not stabilized despite its apparently large value and why a dynamic liquid character persists for a majority spin fraction as $T \rightarrow 0$. Being a very clean system, vesignieite is clearly a good material to address experimentally these pending questions related to the criticality of KAFM physics.

ACKNOWLEDGMENTS

We acknowledge the technical assistance of A. Amato (PSI) and enlightening discussion with A. Zorko. The work was partly supported by Grant ANR-09-JCJC-0093-01, the EU FP-6 Program (Contract No. RII3-CT-2003-505925), and beam time at the ISIS and PSI facilities.

*a.s.wills@ucl.ac.uk

¹R. R. P. Singh and D. A. Huse, *Phys. Rev. Lett.* **68**, 1766 (1992).

²P. Sindzingre and C. Lhuillier, *Europhys. Lett.* **88**, 27009 (2009).

³M. Mambrini and F. Mila, *Eur. Phys. J. B* **17**, 651 (2000).

⁴M. B. Hastings, *Phys. Rev. B* **63**, 014413 (2000).

⁵Y. Uemura *et al.*, *Phys. Rev. Lett.* **73**, 3306 (1994).

⁶Z. Hiroi, M. Hanawa, N. Kobayashi, M. Nohara, H. Takagi, Y. Kato and M. Takigawa, *J. Phys. Soc. Jpn.* **70**, 3377 (2001).

⁷A. Fukaya *et al.*, *Phys. Rev. Lett.* **91**, 207603 (2003).

⁸F. Bert, D. Bono, P. Mendels, F. Ladieu, F. Duc, J.-C. Trombe, and P. Millet, *Phys. Rev. Lett.* **95**, 087203 (2005).

⁹M. A. de Vries, K. V. Kamenev, W. A. Kockelmann, J. Sanchez-Benitez, and A. Harrison, *Phys. Rev. Lett.* **100**, 157205 (2008).

¹⁰M. P. Shores, E. A. Nytko, B. M. Bartlett, and D. G. Nocera, *J. Am. Chem. Soc.* **127**, 13462 (2005).

¹¹R. H. Colman, A. Sinclair, and A. S. Wills, *Chem. Mater.* **23**, 1811 (2011).

¹²S. Chu, T. M. McQueen, R. Chisnell, D. E. Freedman, P. Müller, Y. S. Lee and D. G. Nocera, *J. Am. Chem. Soc.* **132**, 5570 (2010).

¹³R. H. Colman, C. Ritter and A. S. Wills, *Chem. Mater.* **20**, 6897 (2008).

¹⁴R. H. Colman, A. Sinclair, and A. S. Wills, *Chem. Mater.* **22**, 5774 (2010).

¹⁵P. Mendels, F. Bert, M.A. deVries, A. Olariu, A. Harrison, F. Duc, J. C. Trombe, J. Lord, A. Amato, and C. Baines, *Phys. Rev. Lett.* **98**, 077204 (2007).

¹⁶J. S. Helton *et al.*, *Phys. Rev. Lett.* **98**, 107204 (2007).

¹⁷M. A. de Vries, J. R. Stewart, P. P. Deen, J. Piatek, G. N. Nilsen, H. M. Ronnow, and A. Harrison, *Phys. Rev. Lett.* **103**, 237201 (2009).

¹⁸A. Olariu, P. Mendels, F. Bert, F. Duc, J. C. Trombe, M. A. deVries, and A. Harrison, *Phys. Rev. Lett.* **100**, 087202 (2008).

¹⁹F. Bert, S. Nakamae, F. Ladieu, D. LHote, P. Bonville, F. Duc, J. C. Trombe, and P. Mendels, *Phys. Rev. B* **76**, 132411 (2007).

²⁰Y. Okamoto, H. Yoshida, and Z. Hiroi, *J. Phys. Soc. Jpn.* **78**, 033701 (2009).

²¹W.-M. Zhang *et al.*, *J. Phys. Soc. Jpn.* **79**, 023708 (2010).

²²C. Guillemin, C. R. Hebd. Seances Acad. Sci. **240**, 2331 (1955).

²³C.-D. Wu, C.-Z. Lu, X. Lin, S.-F. Lu, H.-H. Zhuang and J.-S. Huang, *J. Alloys Compd.* **368**, 342 (2004).

²⁴We used $P_{\text{nuc}}(t) = f_1 P_{\text{OH}}(\omega, \Delta_{\text{OH}}, t) + f_{23} P_{\text{KT}}(t, \Delta H_{23}) + f_4 P_{\text{KT}}(t, \Delta H_4)$ where f_1 , f_4 , and f_{23} are the fractions of muons stopping close to O1, O4, and to both O2 and O3, which feature extremely similar crystallographic environments. $P_{\text{KT}}(t, \Delta H)$ is the familiar Kubo-Toyabe relaxation function expected for a static field distribution of width ΔH . Muons stopping next to O1 form a $\mu\text{-OH}$ complex, which yields a specific oscillating relaxation.^{15,25} The following values were refined: $f_1 \sim f_{23} \sim f_4 = 0.33(5)$, $\Delta H_{23} = 1.7(1)$ G, $\Delta H_4 = 4.2(1)$ G, $\omega/\gamma_\nu = 4.6(1)$ G and $\Delta_{\text{OH}} = 0.7(3)$ G.

²⁵J. H. Brewer, S. R. Kreitzman, D. R. Noakes, E. J. Ansaldo, D. R. Harshman, and R. Keitel, *Phys. Rev. B* **33**, 7813 (1986).

²⁶A. Keren, J. S. Gardner, G. Ehlers, A. Fukaya, E. Segal, and Y. J. Uemura, *Phys. Rev. Lett.* **92**, 107204 (2004).

²⁷F. Wang, A. Vishwanath, and Y. B. Kim, *Phys. Rev. B* **76**, 094421 (2007).

²⁸O. Cépas, C. M. Fong, P. W. Leung, and C. Lhuillier, *Phys. Rev. B* **78**, 140405 (2008).

²⁹A. Zorko, S. Nellutla, J. vanTol, L. C. Brunel, F. Bert, F. Duc, J. C. Trombe, M. A. deVries, A. Harrison, P. Mendels, *Phys. Rev. Lett.* **101**, 026405 (2008).

³⁰S. El Shawish, O. Cépas, and S. Miyashita, *Phys. Rev. B* **81**, 224421 (2010).